

Supplement of *Clim. Past*, 12, 769–786, 2016
<http://www.clim-past.net/12/769/2016/>
doi:10.5194/cp-12-769-2016-supplement
© Author(s) 2016. CC Attribution 3.0 License.



Climate
of the Past

Open Access

The EGU logo features the letters 'EGU' in a bold, sans-serif font, with a circular arrow graphic behind the 'G'.

Supplement of

The WAIS Divide deep ice core WD2014 chronology – Part 2: Annual-layer counting (0–31 ka BP)

Michael Sigl et al.

Correspondence to: M. Sigl (michael.sigl@psi.ch)

The copyright of individual parts of the supplement might differ from the CC-BY 3.0 licence.

Supplementary Information

A: Main input parameters for the various StratiCounter runs

The algorithm was initialized based on a preliminary set of layer counts in a given depth interval, based on which the general pattern of seasonal influx of the various chemical species (Table 1) was inferred. Representative depth intervals were selected for the various climate periods. Additionally, for each run, the percentage-wise variability of layer thicknesses could either be held constant, or optimized based on the inferred layering in the data. For the upper part, the data contained sufficient information that the algorithm performed well when self-selecting all parameters used for modelling the layer shapes. For the deepest part (2711-2800 m), however, it was necessary to prescribe the percentage-wise variability of individual layer thicknesses.

Table S1. Summary of input variables for the StratiCounter

Depth interval	Initialization interval for algorithm	Percentage-wise layer thickness variability as free variable?
188-577 m	150-550 m	Yes
1300-1780 m	1302-1400 m	Yes
1780-2274 m	1950-2015 m	Yes
2711-2800 m	2710-2725 m	No

B: Cases studies of annual layer interpretation in WD2014

Holocene. Here we show three different ice core sections together with the original individually identified layer boundaries obtained with the three different methods. For the ECM method, circles representing the position of the suggested layer boundaries are displayed on top of the ECM record that was solely used for this interpretation. For the other two methods, all aerosol records have been used conjointly for the layer interpretation. The manual aerosol interpretation results are shown on top of the nssS/Na ratio, and StratiCounter results are shown together with the BC record. Grey bars mark those layers where all three methods resulted in the same interpretation, whereas the yellow bars highlight sections in which one method is disagreeing with the others. Note that the position of the individual annual layer boundaries is slightly shifted between the three different methods (Figs. S1, S2)

owing to the different annual cycles of aerosol deposition in Antarctica (Figs. 2, 3), such that ECM and nssS/Na are nominally summer peaks while BC is an autumn peak. The consensus decision defining the final WD2014 annual layer boundaries is marked with grey triangles on top of the graph.

Fig. S1 shows a 1.5 m long section during the Holocene (approximately 7,500 yr BP) with a mean annual layer thickness of 13 cm. In addition to nssS, Na, nssS/Na and BC we also show nssCa as a proxy for mineral dust. We note one area of disagreement (**A**) just above 1514 m depth, where the ECM interpretation has resulted in an additional layer which do not exist in the manual and StratiCounter layer identifications. A small but rather distinct ECM peak has informed this decision, which would result in two 10 cm thick annual layers above and below. Turning to the aerosol records, the Na record shows some indication of a possible additional layer in favour of an additional year, which is not supported by the nssS BC records. The manual interpreter concluded that the chance of marine biogenic sulphur emissions as well as biomass burning emissions failing to record a year in Antarctica was much smaller than the chance of having a year with 50% higher accumulation and some deposition of sea-salt outside the main season (causing enrichment in Na and ECM). Consequently, the manual interpreter did not interpret an additional year. With the majority of the aerosol records indicating no extra year, the StratiCounter algorithm reached the same conclusion. When later establishing the consensus decision based on examining all available records (ECM and CFA), the three investigators gave more credit to the nssS and BC records. From an atmospheric chemistry perspective, it is much more difficult to explain the absence of a seasonal peak (because emission, transport and depositions are unlikely to fail completely) whereas the occurrence of multiple peaks can be easily explained especially for sea-salt emissions that influence the Na and ECM record. An example how the input of sea-salt aerosols can disturb the ECM records is shown in (**B**) although in this case the annual layer interpretation of the ECM record is in agreement with the other two methods. Finally, this ice-core section also illustrates the rather rare example (**C**) of a secondary peak in BC with a slightly unusual timing that co-occurred with deposition of mineral dust indicated by nssCa. All three methods agreed in the interpretation of this being caused by internal variability, which in the case of the aerosol-based methods benefited from the broad scope of the available tracers.

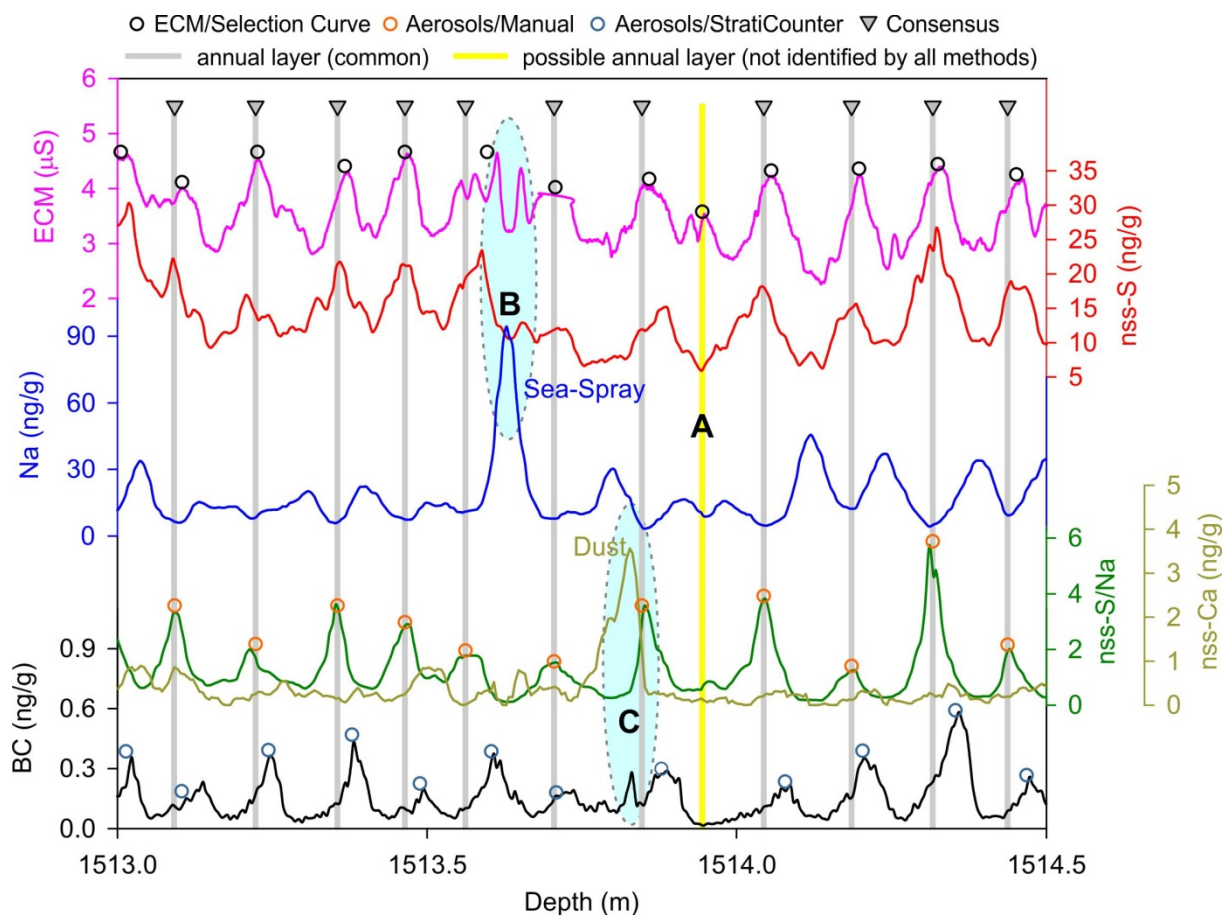


Figure S1. Example of a 1.5 m long ice core section of WAIS Divide (approximately 7,500 years BP) with annual-layer markers (triangles with grey lines) indicated. Also shown are the individual results of the three counting methods ECM (selection curve with manual re-interpretation), manual and StratiCounter interpretation multi-parameter aerosol records (circles). Annual layers for which the layer-counting decisions disagreed between the three methods are highlighted (yellow line), with sections (A-C) discussed in the text.

This case study outlined some of the rationale behind our interpretation processes when performing the annual layer dating, but cannot cover all possibilities. In the end, manual identification as well as consensus decisions of each individual layer is still based on more or less subjective decisions. Overall, as long as the identification is not hampered by low sampling resolution, we prioritized the parameters as $BC > nssS > Na > ECM$ (in the brittle ice: $nssSO_4 > Na > DEP > NO_3$). The strong weighing of the BC record in the decision process makes sense, because these measurements are particulate-bound, so the annual cycle in the firm is not subject to any post-depositional displacements, which could hamper correct annual layer interpretation. It has been shown, for example, in ice cores from Greenland and Antarctica that H_2SO_4 of volcanic origin can cause species such as NO_3^- to move in the ice (by

diffusion in the firm air) leading to increased NO_3 concentrations directly above and below large H_2SO_4 peaks (Clausen et al., 1997; Röthlisberger et al., 2002). This process may also explain the extra peaks and unusual timing of NO_3^- , Na and DEP observed in WDC at 1017 m depth in the direct vicinity of the large nssSO_4 peak (Fig. 4). Here, our decision of not interpreting an extra layer was strongly relying on the absence of an according sulfur peak, supported by a resulting layer thickness in agreement with surrounding layers.

Antarctic Cold Reversal. Fig. S2 shows a 2 m long section during the Antarctic Cold Reversal (approximately 14,700 yr BP) with a mean annual layer thickness of 8 cm. Here, the identified numbers of annual layers using the ECM data and the fully independent manual interpretation of the aerosol records alone are identical, whereas StratiCounter identified four layers less within this section (labelled A-D). Upon inspection, we recognized that particularly those parameters based on ICPMS analyses (e.g., Na, S) appear to no longer provide sufficient resolution to fully resolve all annual layers. Nevertheless, distinctive inflection points in the two different source tracers Na and nssS (**A**) in combination with a clear BC peak lead the manual interpreter to the annual layer decision. For the layer (**B**), the decision was similarly predominantly done on the basis of the distinctive BC peak, as the layering in all other tracers is disturbed by volcanic acid deposition. Both these examples show how the StratiCounter algorithm can be led astray by volcanic influence on the records because in contrast to a manual interpreter, the algorithm has no knowledge that volcanic eruptions may disturb the layer signals. In the manual interpretation, layer (**C**) was deemed by the investigator the least certain of all layers within this section. There are small inflection points in the Na and nssS/Na records and the BC concentrations are comparably high so that an additional smaller BC peak could be masked by the broad BC signal from the previous year (to the right). In this section, the layer thickness was the pivotal argument for the layer decision in the manual interpretation, although nor do these exclude the possibility of this layer boundary being erroneous. Finally, in layer (**D**) a small but distinctive BC peak together with weak double peaks in nssS and nss-S/Na were manually interpreted as evidence in favour of a layer. In contrast, StratiCounter considered the evidence for this to be too weak, and decided not to place a layer here. All four cases in which the manual interpretation differed from the StratiCounter results, there were comparably clear signals in the ECM. When performing the consensus decision, they were therefore all finally interpreted as annual layers in WD2014. It is not entirely surprising that the objective StratiCounter was

interpreting too few layers in the deeper part, because 7 of the 8 parameters that the algorithm is using (all except BC) is based on ICPMS data providing the lowest sampling resolution.

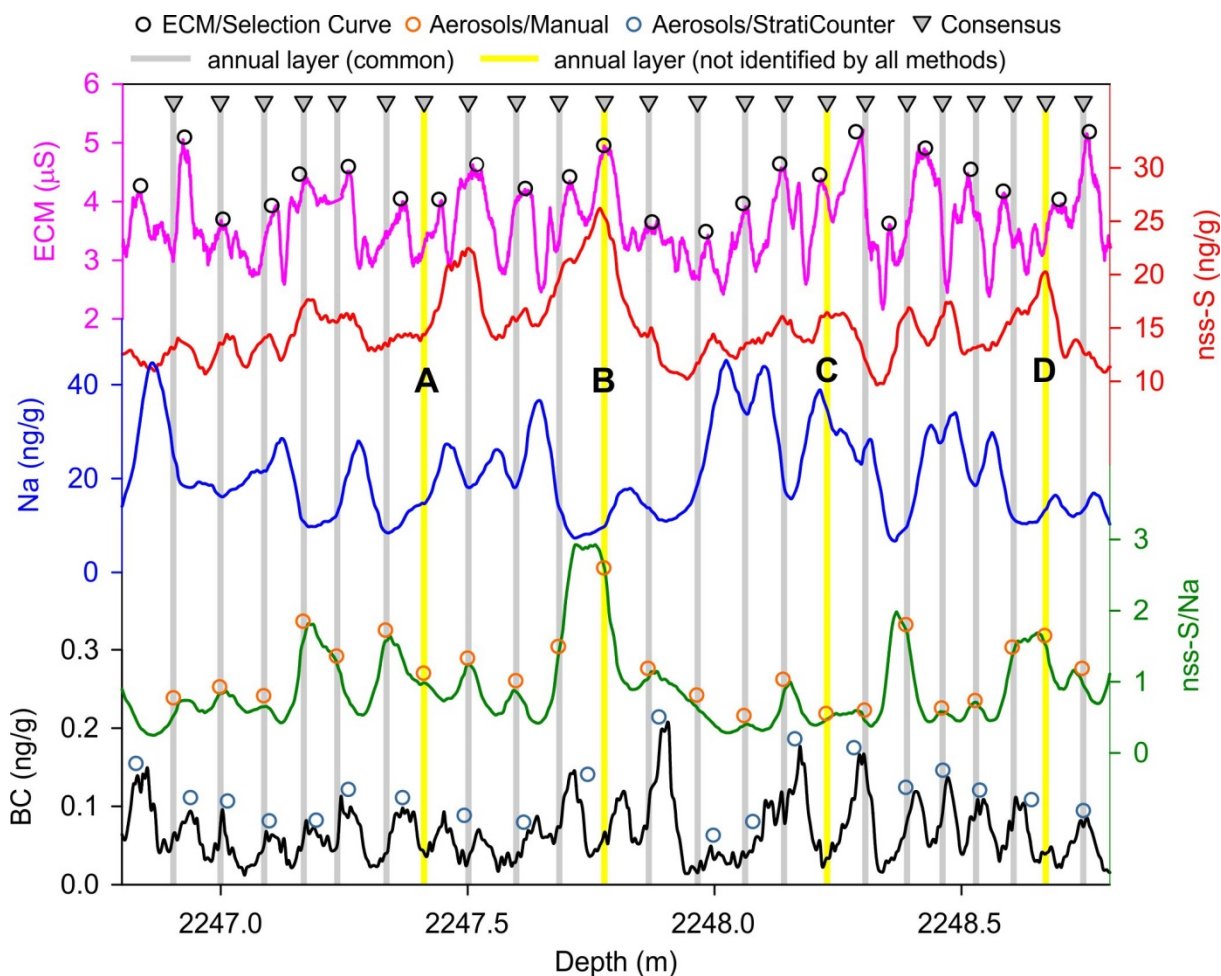


Figure S2. Example of a 2 m long ice core section of WAIS Divide (approximately 14,700 years BP) with annual-layer markers (triangles with grey lines) indicated. Identical to Fig. 6, but with individual layer counting results for the three different methods indicated.

Overall, this case study outlined the rationale of our layer decision process in the deeper part where we still have multiple-parameter records but where limitations start to arise owing to the reduced time-resolution of the data. Within this section we weighed the manual aerosol interpretation of BC stronger than all other aerosol records, and gave within the consensus interpretation also a strong weight to the ECM record, which provides the highest resolution measurements.

End of the annual layer interpretation. There was no exact demarcation of where annual layers were no longer interpretable. We stopped the annual layer interpretation when we were no longer confident that all years were being resolved. During the manual interpretation of the

ECM, the difficulty in identifying annual layers notably increased between 2850 m and 2900 m (Fig. S3). The increased difficulty was associated with broadening of peaks and troughs such that the annual layer thickness appears to be increasing in short sections while the annual layer thickness remained smaller in nearby sections. Even though the vast majority of annual layers remained identifiable, an increasing number of annual layers appeared to not be resolved. Therefore, we terminated the interpretation at 2850 m, just older than DO 5.1 which provided a tie-point to transition to the stratigraphic dating of the lower part of the WAIS Divide core (Buizert et al., 2015).

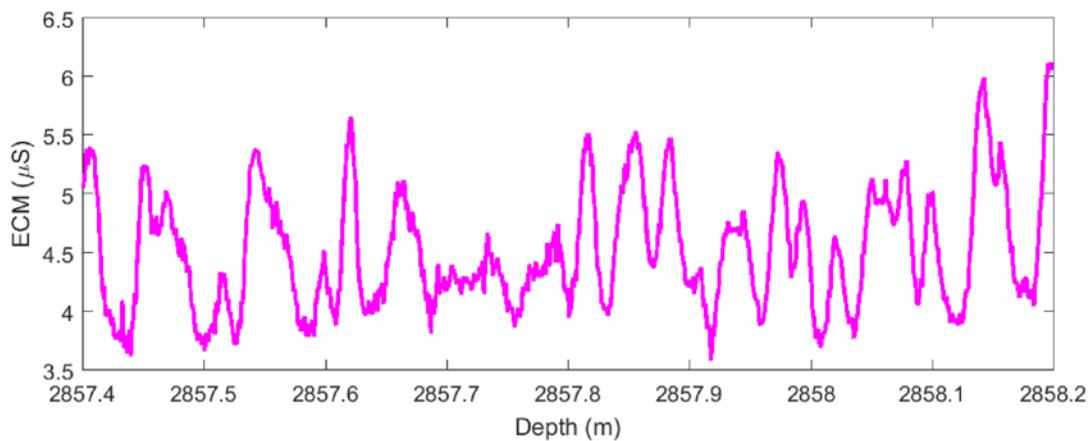


Figure S3. ECM data illustrating why the annual layering interpretation was stopped at 2850 m. Annual layering is visible below 2857.8 m. Above 2857.8 m, the annual layering is obscured by sections with little variation (2857.7-2857.8 m) or broad peaks (e.g. 2857.55 m), causing the annual layer interpretation to be unreliable.

C: Assumptions and uncertainties in the synchronicity of Greenland $\delta^{18}\text{O}$, Hulu $\delta^{18}\text{O}$ and WDC CH_4 during rapid warming events

Speleothems in the Alps and other parts of Europe clearly show DO events as abrupt changes in calcite $\delta^{18}\text{O}$ (Luetscher et al., 2015; Moseley et al., 2014; Spötl et al., 2006). Atmospheric models suggest that any DO abrupt change recorded in Greenland should be essentially synchronous with European stalagmites (Pausata et al., 2011). So there is generally broad agreement that European stalagmites are unquestionably synchronous at the level of several decades or less. This “several decades” figure comes from the models. In fact most of the change happens in one year, but several decades is a conservative figure that allows for the well-known unforced variability in the climate system. So the real question is, are European stalagmite DO signals synchronous with Chinese cave stalagmite DO signals? Here the

models again show that they are synchronous within several decades. The physics of this teleconnection are not as well understood as the Greenland-Europe one, but probably have to do with the southward shift of the wintertime westerlies during a Greenland Stadial when much of the North Atlantic ocean is covered with sea ice. This is indeed what the models show (Pausata et al., 2011). The cold winter air travels across the Mediterranean, over the Arabian peninsula, and across the northern Indian ocean, where it cools the ocean substantially. Because of the thermal memory of the ocean, this cool anomaly persists into the following summer, when it causes a weak monsoon. The link between north Indian ocean SST and the strength of the Asian monsoon is well documented and makes good physical sense. During an interstadial, by contrast, the winter westerlies go across the Asian land mass. Land does not have the thermal memory that the ocean does, so the following summer's monsoon is not as affected. All of these physical processes have inherent timescales of a few decades or less, the time it takes to warm and cool the upper ocean. So from first principles and physics we would expect the Chinese caves to lag European caves by no more than several decades.

Another test of the hypothesis of synchronicity comes from the fine structure of the Chinese cave $\delta^{18}\text{O}$ and Greenland $\delta^{18}\text{O}$ and calcium records. Both contain astonishingly high resolution structure on timescales of a century or less, that is virtually identical in its frequency content (see Fig. 5 and Fig. 6 in Buizert et al., 2015). We know a priori that realistic physical processes in the climate system, that cause lags, also cause smoothing - i.e. loss of high frequency content. For example, warming of the ocean acts as an integrator resulting in a lag of ocean temperature behind Greenland temperature, and a loss of high frequency signals in the ocean temperature record. Therefore, we would expect a reduction of the high-frequency content in Chinese caves if there were a substantial lag. More precisely, century-scale oscillations in Chinese caves should be substantially damped in amplitude if there were a century-scale lag of China behind Greenland. The records in fact show no such loss of high frequencies. The sampling resolution of the new Hulu $\delta^{18}\text{O}$ record is about 10 years, and the frequency content of this record is not significantly different from that of the Greenland calcium and $\delta^{18}\text{O}$ records, when those records have been resampled at 10-year spacing to mimic the Hulu sample spacing.

A further test comes from the methane itself. Modern observations confirm that the Asian monsoon region is an important contributor to the global methane budget (Xiong et al., 2009;

Xiong et al., 2010). Based on this reasoning, and bottom-up models of vegetation and methane production that show response times of a few decades or less to abrupt changes in monsoon rainfall, one expects that methane change could be a proxy for the timing of monsoon rainfall change. In fact, the well-known observation from Greenland ice core methane and $\delta^{15}\text{N}$ records (Severinghaus et al., 1998) is indeed that abrupt change in methane concentration during DO events lags behind Greenland $\delta^{18}\text{O}$ and calcium by 30 yr or less typically (when measured as the lag of methane's mid-point behind $\delta^{18}\text{O}$'s and calcium's midpoint). Note that Rosen et al., (2014) did not measure this lag. Rosen et al., (2014) measured the phasing of the onset or inflection point at the beginning of the methane rise and the beginning of the temperature (i.e. $\delta^{15}\text{N}$) rise, finding that they were synchronous within uncertainty, with a most-probable lag of methane's onset by 5 years.

Greenland methane and $\delta^{15}\text{N}$ phasing has not only been measured except by Rosen et al., (2014), but Baumgartner et al., (2014) also did an extensive study of this phasing for most of the DO events. We estimate that about 17-20 of the DO events have had their methane-d15N phasing measured.

The overall conclusion of this methane-based test is that DO events caused changes in methane production within several decades following Greenland warming. It seems unlikely that Chinese methane sources somehow lagged the pulse of methane production elsewhere. If they did, there ought to be delayed increases in methane concentration observed in the record, but these are not observed. Instead the methane shoots up to an apparently stable Interstadial value within typically 50 yr. To summarize, the hypothesis that fits the data best, is that Chinese methane sources responded synchronously with all other low-latitude sources.

D: Comparison to a speleothem chronology from Europe

Based on the assumptions outlined above we also compare WD2014 based ages for rapid NH warming events to those from new stalagmite $\delta^{18}\text{O}$ composite record from the European Alps (H7) which provides exceptionally precise U/Th dates (± 50 years on average, 2σ) for these events. To account for the lag in WDC methane relative to H7 $\delta^{18}\text{O}$ mid-points we applied the same phasing correction as was applied for the comparison to Greenland ice-core $\delta^{18}\text{O}$ (see Table 4, Table S2).

Our estimates for rapid warming events based on WD2014 are different from the precisely U/Th dated Alpine cave records on average by less than 20 years at three different time

windows during the past 30,000 years (Fig. S4, Table S2). This independent test provides independent additional confirmation of the high level of dating accuracy of WD2014.

Table S2. Comparison of WD2014 based estimates of North Atlantic climate transitions with those from the high-precision alpine speleothem record Sieben Hengste 7H (Luetscher et al., 2015).

Climate Transition	WD2014 (Antarctica)		Sieben Hengste 7H (Alps)		
	Gas age (BP 1950)	Mid-point lag (yr)	Transition age (BP1950)	U/Th age (BP1950)	Error (2 σ) (yr)
OD-BA	14576	+45	14621	14644	40
DO 3 (onset)	27755	+25	27780	27802	54
DO 4 (onset)	29011	+25	29036	29047	66

We used the GICC05 chronology to which age comparisons have previously been made for 7H (Luetscher et al., 2015) and WD2014 (this study) to align WD2014 and 7H. We assume the same phasing relationship between WDC CH₄ mid-point and H7 mid-point than was used for the comparison with NGRIP ($\delta^{18}\text{O}$).

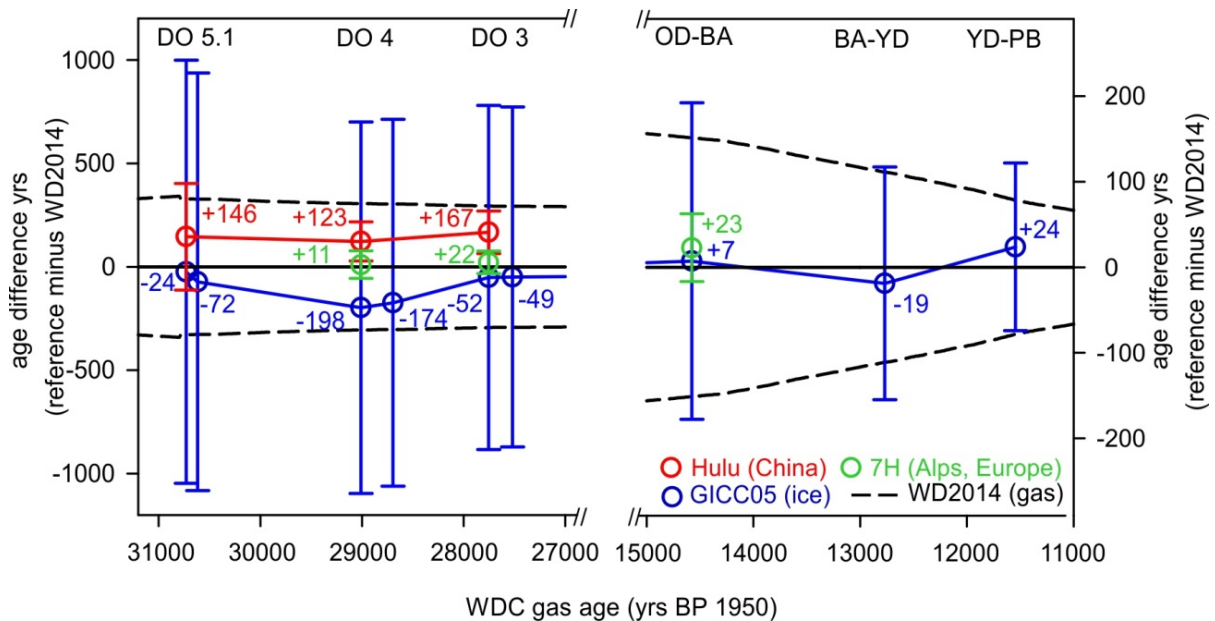


Figure S4. Comparison between WD2014 and three independently-dated records from the Northern Hemisphere. As Figure 10, but also showing age differences between WD2014 and 7H cave in the European Alps (Luetscher et al., 2015) using CH₄ synchronization for time periods of rapid climate transition (i.e., NGRIP $\delta^{18}\text{O}$, Hulu and 7H $\delta^{18}\text{O}$ calcite) between 31 and 27 ka BP (left panel) and between 15 and 11 ka BP (right panel). See Fig. 10 for additional details.

Supplementary References

- Baumgartner, M., Kindler, P., Eicher, O., Floch, G., Schilt, A., Schwander, J., Spahni, R., Capron, E., Chappellaz, J., Leuenberger, M., Fischer, H., and Stocker, T. F.: NGRIP CH₄ concentration from 120 to 10 kyr before present and its relation to a delta N-15 temperature reconstruction from the same ice core, *Clim Past*, 10, 903-920, 2014.
- Buizert, C., Cuffey, K. M., Severinghaus, J. P., Baggenstos, D., Fudge, T. J., Steig, E. J., Markle, B. R., Winstrup, M., Rhodes, R. H., Brook, E. J., Sowers, T. A., Clow, G. D., Cheng, H., Edwards, R. L., Sigl, M., McConnell, J. R., and Taylor, K. C.: The WAIS Divide deep ice core WD2014 chronology - Part 1: Methane synchronization (68-31 kaBP) and the gas age-ice age difference, *Clim Past*, 11, 153-173, 2015.
- Clausen, H. B., Hammer, C. U., Hvidberg, C. S., DahlJensen, D., Steffensen, J. P., Kipfstuhl, J., and Legrand, M.: A comparison of the volcanic records over the past 4000 years from the Greenland Ice Core Project and Dye 3 Greenland Ice Cores, *J Geophys Res-Oceans*, 102, 26707-26723, 1997.
- Luetscher, M., Boch, R., Sodemann, H., Spötl, C., Cheng, H., Edwards, R. L., Frisia, S., Hof, F., and Muller, W.: North Atlantic storm track changes during the Last Glacial Maximum recorded by Alpine speleothems, *Nat Commun*, 6, 2015.
- Moseley, G. E., Spötl, C., Svensson, A., Cheng, H., Brandstatter, S., and Edwards, R. L.: Multi-speleothem record reveals tightly coupled climate between central Europe and Greenland during Marine Isotope Stage 3, *Geology*, 42, 1043-1046, 2014.
- Pausata, F. S. R., Battisti, D. S., Nisancioglu, K. H., and Bitz, C. M.: Chinese stalagmite delta O-18 controlled by changes in the Indian monsoon during a simulated Heinrich event, *Nat Geosci*, 4, 474-480, 2011.
- Rosen, J. L., Brook, E. J., Severinghaus, J. P., Blunier, T., Mitchell, L. E., Lee, J. E., Edwards, J. S., and Gkinis, V.: An ice core record of near-synchronous global climate changes at the Bolling transition, *Nat Geosci*, 7, 459-463, 2014.
- Röthlisberger, R., Hutterli, M. A., Wolff, E. W., Mulvaney, R., Fischer, H., Bigler, M., Goto-Azuma, K., Hansson, M. E., Ruth, U., Siggaard-Andersen, M. L., and Steffensen, J. P.: Nitrate in Greenland and Antarctic ice cores: a detailed description of post-depositional processes, *Annals of Glaciology*, Vol 35, 35, 209-216, 2002.
- Severinghaus, J. P., Sowers, T., Brook, E. J., Alley, R. B., and Bender, M. L.: Timing of abrupt climate change at the end of the Younger Dryas interval from thermally fractionated gases in polar ice, *Nature*, 391, 141-146, 1998.
- Spötl, C., Mangini, A., and Richards, D. A.: Chronology and paleoenvironment of Marine Isotope Stage 3 from two high-elevation speleothems, *Austrian Alps, Quaternary Sci Rev*, 25, 1127-1136, 2006.
- Xiong, X., Houweling, S., Wei, J., Maddy, E., Sun, F., and Barnet, C.: Methane plume over south Asia during the monsoon season: satellite observation and model simulation, *Atmos Chem Phys*, 9, 783-794, 2009.
- Xiong, X. Z., Barnet, C. D., Zhuang, Q. L., Machida, T., Sweeney, C., and Patra, P. K.: Mid-upper tropospheric methane in the high Northern Hemisphere: Spaceborne observations by AIRS, aircraft measurements, and model simulations, *J Geophys Res-Atmos*, 115, 2010.